DNA Research, 2018, 25(1), 71–86
doi: 10.1093/dnares/dsx039
Advance Access Publication Date: 3 October 2017
Full Paper

OXFORD

Full Paper

Circular RNAs are abundant and dynamically expressed during embryonic muscle development in chickens

Hongjia Ouyang[1,2], Xiaolan Chen[1,2], Zhijun Wang[1,2], Jiao Yu[1,2], Xinzheng Jia[1,2], Zhenhui Li[1,2], Wei Luo[1,2], Bahareldin Ali Abdalla[1,2], Endashaw Jebessa[1,2], Qinghua Nie[1,2,*], and Xiquan Zhang[1,2]

[1]Department of Animal Genetics, Breeding and Reproduction, College of Animal Science, South China Agricultural University, Guangzhou 510642, Guangdong, People's Republic of China, and [2]Guangdong Provincial Key Lab of Agro-Animal Genomics and Molecular Breeding, and Key Lab of Chicken Genetics, Breeding and Reproduction, Ministry of Agriculture, Guangzhou 510642, Guangdong, People's Republic of China

*To whom correspondence should be addressed. Tel. +86 20 85285759. Fax. +86 20 85280740. Email: nqinghua@scau.edu.cn

Edited by Dr. Osamu Ohara

Received 22 January 2017; Editorial decision 6 September 2017; Accepted 7 September 2017

Abstract

The growth and development of skeletal muscle is regulated by proteins as well as non-coding RNAs. Circular RNAs (circRNAs) are universally expressed in various tissues and cell types, and regulate gene expression in eukaryotes. To identify the circRNAs during chicken embryonic skeletal muscle development, leg muscles of female Xinghua (XH) chicken at three developmental time points 11 embryo age (E11), 16 embryo age (E16) and 1 day post hatch (P1) were performed RNA sequencing. We identified 13,377 circRNAs with 3,036 abundantly expressed and most were derived from coding exons. A total of 462 differentially expressed circRNAs were identified (fold change >2; q-value <0.05). Parental genes of differentially expressed circRNAs were related to muscle biological processes. There were 946 exonic circRNAs have been found that harbored one or more miRNA-binding site for 150 known miRNAs. We validated that circRBFOX2s promoted cell proliferation through interacted with miR-206. These data collectively indicate that circRNAs are abundant and dynamically expressed during embryonic muscle development and could play key roles through sequestering miRNAs as well as other functions.

Key words: circular RNA, chicken, skeletal muscle, embryonic development, cell proliferation

1. Introduction

Non-coding RNA such as microRNAs (miRNA) and long non-coding RNAs exist in many cells and regulate gene expression and possibly perform other biological functions.[1–5] Circular RNAs are a novel non-coding RNA that forms a covalently closed continuous loop and have been observed for decades in plant viroids[6] and in a few mammalian genes.[7–10] CircRNAs were generally considered to be splicing artifacts or by-products until recent advances in RNA-sequencing (RNA-seq) technology.[11] CircRNAs are served as a new class of RNAs that have been identified widespread in eukaryotic tissues and cells from humans, mice, nematodes, fruit flies and plants.[12–19]

CircRNAs can arise from exons, introns, untranslated regions, non-coding RNA loci as well as intergenic and antisense transcripts.

They are abundantly and widely expressed in eukaryotes, and often show tissue and developmental stage-specific expression patterns.[12,15,20] In some genes, circular RNA isoforms are even more abundant than their linear counterparts.[21] CircRNAs are also expressed across eukaryotes, and in humans, hundreds of exonic circRNAs are found to be with circular orthologues in murine.[18–22]

The biological functions of circRNA are still largely unknown but they are implicated in the regulation of gene expression at multiple levels. Some exonic circRNAs (eciRNA) can function as miRNA sponges, which compete with mRNAs for miRNA binding and thus up-regulate the expression of miRNAs target gene. One representative example is the cerebellar degeneration-related 1 antisense transcript (*CDR1as*) that contains over 60 conserved miR-7 target sites.[13,14] A *CDR1as* knockdown leads to reduced expression of mRNAs containing miR-7-binding sites. Overexpression of *CDR1as* has an effect similar to a miR-7 knockdown and this impaired midbrain development in zebrafish.[13] Circular RNAs can regulate transcription *via* RNA Pol II interactions and have been demonstrated for the ciRNA (intronic circular RNA) *ci-ankrd52* and *ci-sirt7*.[23] EIciRNAs (exon-intron circular RNA) regulate their parental genes through interaction with the spliceosome component U1 snRNP (small nuclear ribonucleoprotein).[24] CircRNA biogenesis may also compete with pre-mRNA splicing and thus regulate linear mRNA levels.[25] In addition, some circRNAs have been found to serve as templates for coding peptides or proteins, especially in that modified by N6-methyladenosine or with the presence of internal ribosomal entry sites (IRES).[26–29]

Skeletal muscle is the most important component of food animals and directly correlates with meat quantity and quality. The growth and development of skeletal muscle involves a series of very complex biological process, regulated by many signaling pathways, genes, transcription factors and ncRNAs.[30–33] CircRNAs can play important roles in biologic processes as well as human disease.[34–36] CircRNAs also have been identified abundantly expressed in monkey skeletal muscle and may play key roles in growth and development.[37] In this study, we identified circRNAs during chicken embryonic skeletal muscle development by RNA sequencing to explore the functions of circRNAs in chicken skeletal muscle.

2. Materials and methods

2.1. Ethics standards

Animal experiments were handled in compliance and all efforts were made to minimize suffering. It was approved by the Animal Care Committee of South China Agricultural University (Guangzhou, China) with approval number SCAU#0014.

2.2. Samples for circular RNA sequencing

A total of 240 XH chickens of E10 embryonic age were obtained from the Chicken Breeding Farm of South China Agricultural University (Guangzhou, China), and incubated in Automatic Incubator (Oscilla, Shandong, China) at 37.8 °C, with 60 ± 10% humidity. During E10 to 1 day post hatch (P1), leg muscles of 20 XH chickens were collected daily. The sex of chicken embryo was identified by PCR of the *CHD1* gene.[38] Leg muscles of female XH chickens at E11, E16 and P1 were used for circular RNA sequencing.

2.3. Circular RNA library construction and Illumina sequencing

Total RNAs of six female chickens (E11, E16, and P1; each stage two individuals), were isolated by using Trizol reagent (Invitrogen, Carlsbad, CA, USA) and then treated with DNase (Promega, Madison, WI, USA) following the manufacturer's instructions. The quantity and quality of RNAs were evaluated by Nanodrop2000 (Thermo, Waltham, MA, USA) and gel electrophoresis. Total RNA samples (5 μg) were treated with the Ribo-Zero-magnetic-kit (Epicenter, Madison, Wisconsin, USA) to remove rRNA, and then digested with 20 U of RNase R (RNR07250, Epicenter). RNA-Seq libraries were prepared using the Tru Seq RNA LT Sample Prep Kit v2 (Illumina, San Diego, CA, USA) following the manufacturer's instructions. The libraries were sequenced using an Illumina Hiseq 3000 instrument with a Paired-End module (at a depth of 50 million reads) at Genergy Biotechnology Co., Ltd. (Shanghai, China).

2.4. Annotation of chicken circRNAs

All sequencing data are available in the Gene Expression Omnibus (GEO) with accession number (GSE89355). For all raw sequencing data of each sample, adapter reads and low-quality reads were removed using Trim Galore (http://www.bioinformatics.babraham.ac.uk/projects/trim_galore/ (16 September 2017, date last accessed)). The filtered data were mapped to the chicken genome (Gallus_gallus-4.0/galGal4) using TopHat software.[39] The mapping reads was performed transcript assembly using Cufflinks software.[40] Identification of circRNAs was performed using CIRI.[41]

2.5. Differential expression analysis

Expression levels of circRNAs were quantified using the number of reads spanning back-spliced junctions (circular reads). The relative expression of circRNAs was denoted as BSRP (back-spliced reads per million mapped reads), using circular reads normalized to per million mapped reads. Differentially expressed circRNAs among three groups (E11, E16 and P1) were identified using the DESEQ software package (http://www.bioconductor.org/packages/release/bioc/html/DEGseq.html (16 September 2017, date last accessed)) with a t test q-value < 0.05 and fold change > 2. The top 200 expressed circRNAs were log2 transformed, gene mean centered and visualized as heatmaps using the Multi Experiment Viewer (http://www.tm4.org/ (16 September 2017, date last accessed)).

2.6. Target miRNA prediction, pathway and network analysis

All exonic circRNAs were used to predict miRNAs potential binding sites using miRanda (http://www.microrna.org/microrna/home.do (16 September 2017, date last accessed)) with threshold parameters as follows: single-residue-pair match scores > 140, $\Delta G < -10$ kcal/mol and demand strict 5' seed pairing. All parental genes of differentially expressed circRNAs were subjected to Gene Ontology (GO) (http://www.geneontology.org/ (16 September 2017, date last accessed)) and KEGG (http://www.genome.jp/kegg/ (16 September 2017, date last accessed)) pathway enrichment analysis using DAVID 6.7 Functional Annotation Tool (http://david.abcc.ncifcrf.gov/ (16 September 2017, date last accessed)). All parental genes of circRNAs were set as the background gene list. Gene network analysis was performed by Ingenuity Pathways analysis (IPA; Ingenuity Systems; http://www.ingenuity.com (16 September 2017, date last accessed)).

2.7. Validation of circRNAs by Sanger sequencing

The circRNAs were validated using PCR with divergent and convergent primers as previously described.[22] Divergent primers were designed in regions about 100 bp from a junction, and convergent

primers were designed in regions of one exon (Details of primers are summarized in Supplementary Table S1). To confirm the junction sequence of circRNAs, PCR products of divergent primers were gel purified and submitted for Sanger sequencing at Sangon Biotech Co. Ltd (Shanghai, China).

2.8. cDNA synthesis and quantitative real-time PCR (qRT-PCR)

Total RNA was used for reverse transcription using RevertAid First Strand cDNA Synthesis Kit (Fermentas, Waltham, MA, USA) with either random hexamers or specific primers for miRNAs as indicated. The relative expression levels of circRNAs or miRNAs were determined by qRT-PCR using SsoFast Eva Green Supermix (Bio-Rad, Hercules, CA, USA) in a final volume of 20 µl. To check the sensitivity of circRNA to RNaseR, qRT-PCR was also performed using RNA samples with and without RNaseR treatment. Primers used for circRNAs were designed as divergent primers to detect backsplice junctions, and bulge-loop primers were synthesized by Ribobio (Guangzhou, China) for miRNAs (Details of primers are summarized in Supplementary Table S1). The *β-actin* gene was used as reference genes for circRNAs, and U6 snRNA was used as reference gene for miRNAs. The qRT-PCR program was performed in a BIO-RAD CFX96 system as follows: 95 °C for 3 min; 40 cycles of 95 °C for 10 s, annealing temperature (58–62 °C) for 30 s, and 72 °C for 30 s; and 72 °C for 1 min. The relative expression level of miRNA was calculated using the comparative $2^{-\Delta Ct}$ ($\Delta Ct = Ct_{target\ gene} - Ct_{reference\ gene}$). Fold change values were calculated using the comparative $2^{-\Delta\Delta Ct}$, in which $\Delta\Delta Ct = \Delta Ct$ (target sample) $- \Delta Ct$ (control sample). All reactions were run in triplicate and presented as means ± S.E.M. The Student's *t*-test was used to compare expression levels among different groups.

2.9. Vector construction and RNA oligonucleotides

The perfect match sequence of gga-miR-1a-3p° or gga-miR-206 was synthesized and cloned into the psiCHECK-2 vector (Promega) using the *NotI* and *XhoI* restriction sites. The circRNA overexpression vectors were constructed using the linear sequences of *circRBFOX2.2-3* and *circRBFOX2.2-4* amplified from chicken leg muscle cDNA using PCR. They were then cloned into pCDciR2.1vector (Supplementary Fig. S1, Geneseed Biotech, Guangzhou, China) according to the manufacturer's protocol using the *KpnI* and *BamHI* restriction sites. The wild type and mutated 3'UTRs sequences of CCND1, CCND2, PAX7 and HDAC4 were synthesized and cloned into the pmirGLO dual-luciferase reporter vector (Promega) using the *NheI* and *XhoI* restriction sites. The exon2-3 or exon2-4 of RBFOX2 were synthesized and cloned into the pcDNA3.1+ vector (Invitrogen) using the *NheI* and *SalI* restriction sites. Small interfering RNA (siRNA) of circRNAs (sequences are summarized in Supplementary Table S1), miRNA mimics and inhibitors were synthesized by Ribobio.

2.10. Cell culture and transfection

Chicken primary myoblasts were isolated from the leg muscles of E11 chickens. Leg muscle (1 g) was minced into sections of approximately 1 mm with scissors and digested with 0.25% trypsin (Gibco, Grand Island, NY, USA) at 37 °C in a shaking water bath (90 oscillations/min). Digestions were terminated by adding foetal bovine serum (Gibco) after 30 min. The mixture was filtered through a nylon mesh with 70 µm pores (BD Falcon). The filtered cells were centrifuged at 350g for 5 min, and maintained in Dulbecco's modified Eagle medium (DMEM) (Gibco), supplemented with 20% foetal bovine serum, and 0.2% penicillin/streptomycin (Invitrogen, Carlsbad, CA, USA) at 37 °C in a 5% CO_2, humidified atmosphere. Serial plating was performed to enrich myoblasts and remove fibroblasts. DF-1 cells were cultured in DMEM with 10% foetal bovine serum and 0.2% penicillin/streptomycin. QM-7 cells were cultured in high-glucose M199 medium (Gibco) with 10% foetal bovine serum, 10% tryptose phosphate broth solution (Sigma, Louis, MO, USA) and 0.2% penicillin/streptomycin. Cells were transfected with 50 nM of miRNA mimics, 100 nM of miRNA inhibitors, 100 nM of siRNA or plasmid (1 µg/ml) using Lipofectamine 3000 reagent (Invitrogen) according to the manufacturer's instructions.

2.11. Luciferase reporter assay and Northern blot analysis

DF-1 cells were seeded in 96-well plates and co-transfected with the dual-luciferase reporter (psiCHECK-2) and miRNA mimics or NC (negative control) and with circRNA overexpression vector, circRNA mutated vector or empty vector (EV) using Lipofectamine 3000 reagent. After transfection for 48 h, the luminescent signals of *firefly* and *Renilla* luciferase were detected using Dual-GLO Luciferase Assay System Kit (Promega) with a Fluorescence/Multi-Detection Microplate Reader (Biotek,Winooski, VT, USA). Northern blotting for miR-206 and U6 were performed with MiRNA Northern Blot Assay Kit (Signosis, Santa Clara, CA, USA) following the manufacturer's instructions.

2.12. Flow cytometry analysis of the cell cycle

After transfection 48 h, myoblasts were collected and fixed in 70% ethanol overnight at −20 °C. The cells were incubated with 50 µg/ml propidium iodide (Sigma), 10 µg/ml RNaseA (Takara) and 0.2% (v/v) Triton X-100 (Sigma) for 30 min at 4 °C. Analyses were performed using a BD AccuriC6 flow cytometer (BD Biosciences, San Jose, CA, USA) and FlowJo (v7.6) software (Treestar Incorporated, Ashland, OR, USA).

2.13. EdU assay

QM-7 cells were seeded in 12-well plates, and at 80% confluence, cell were transfected with overexpression vector or siRNA of circRNAs, miRNA mimic, miRNA inhibitor or negative control. After transfection for 36 h, cell proliferation was tested using a Cell-Light EdU Apollo 567 in Vitro Flow Cytometry Kit (Ribobio). The cells were first incubated with 50 µM EDU for 2 h at 37 °C, and then fixed in 4% paraformaldehyde for 30 min and permeabilized with 0.5% Triton X-100. The proliferating cells were stained with Apollo Dye Solution and Hoechst 33342 (used as control). The EdU-stained cells were visualized by fluorescence microscopy (Nikon, Tokyo, Japan). The cell proliferation rate was calculated using images of randomly selected fields obtained from the fluorescence microscope. We performed four repeats for each group, and three images were used to calculate the cell proliferation rate in each repeat.

2.14. Histology

The leg muscle samples were fixed in 4% paraformaldehyde for a minimum of 24 h and then embedded in paraffin and 10-mm thick serial sections were made. The sections were then subjected to H-E staining following standard protocols. Images were taken using a Moticam 2306 CCD imaging system (Motic Instruments, CA, USA).

2.15. RNA immunoprecipitation and biotin-coupled miRNA pull down

RIP experiments were performed by using the Magna RIP RNA-Binding Protein Immunoprecipitation Kit (Millipore, Bedford, MA) following the manufacturer's instructions. Immunoprecipitation of AGO2 was performed in QM7 cells co-transfected with circRBFOX2s expression vector and miR-1a-3p°, miR-206 or miR-203 control. The mRNA levels of circRBFOX2s were quantified by qRT–PCR and were normalized to *GAPDH* gene. The relative immunoprecipitate/input ratios are plotted.

The 3' end biotinylated miR-1a-3p°, miR-206 or miR-203 mimic (RiboBio) were transfected into QM7 cells along with circRBFOX2s expression vector. The biotin-coupled RNA complex was pull-downed by Dynabeads MyOne Streptavidin C1 kit (Invitrogen) following the manufacturer's instructions. RNA bound to the beads (pull-down RNA) was isolated using Trizol LS reagent (Invitrogen). The mRNA levels of circRBFOX2s in the streptavidin captured fractions were quantified by qRT–PCR and the enrichment ratios of the miR-1a-3p° or miR-206 to the miR-203 control were plotted.

3. Results and discussion

3.1. Overview of circular RNA deep sequencing data

In recent years, a number of reports demonstrated that circRNAs were widespread and abundant existed in various eukaryotes, especially in mammals. However, little information is known regarding circRNAs in domestic animals with the exception of brain cortex of pig[42] and mammary gland tissues of cattle.[43] Here, we performed the genome-wide identification and potential function analysis of circRNAs in chickens. The total number of muscle fibers is the determining factor in muscle mass and this is regulated during embryogenesis or early post hatch in chickens.[44,45] To identify the circRNA during the chicken embryonic skeletal muscle development, leg muscle tissues of two female XH chicken for each at days E11, E16 and P1 were used for RNA sequencing after rRNA-depletion and RNase R treatment (Supplementary Fig. S2). The sex of XH chicken embryos was identified (Supplementary Fig. S3A) and leg muscle tissues of female chickens were performed using hematoxylin-eosin (H-E) staining to visual the muscle fibers during 10 embryo age to post hatch (Supplementary Fig. S3B).

For RNA-seq, a total of about 750 million reads were generated from all six samples, and each sample yielded more than 100 million reads. Raw data were processed to remove adapter and low quality sequences, and then mapped to the chicken reference genome (Gallus_gallus-4.0/galGal4) (Supplementary Table S2). The mapping reads were uniformly distributed in each chromosome, except the abundance in the chromosome MT is much larger than that of the other chromosomes (Fig. 1A).From the six muscle tissues, a total of 13,377 circRNAs were detected; 7,914 in E11, 10,949 in E16, and 9,309 in P1, and 5,176 were detected in all three stages (Fig. 1B and Supplementary Table S3) using the CIRI algorithm method.[41] These results agree with the scope and abundance of circRNAs that have been identified in mammals.[18,21] According to their genomic locus, the chicken circRNAs were grouped as exon (including 5'UTR, 5'UTR-CDS, CDS-3'UTR, 3'UTR and 5'UTR -CDS-3'UTR), intron, exon-intron, intergenic regions or others. Although circRNAs can arise from almost any location in a genome, they are most originate from coding exons.[13,17–19] We also found 11,064 of 13,377 circRNAs were derived from known chicken genes, especially in coding DNA sequences (CDS) ($n = 8{,}110$). The other circRNAs were derived from introns, exon-introns, intergenic regions or other regions (Fig. 1C). All these circRNAs were originated from 3,589 chicken genes. Among them, 1,555 parental genes generated only one circRNA, and the other genes could yield two or more circular isoforms, even smaller fractions yielded more than ten distinct circular isoforms (Fig. 1D), similar to the results in pigs.[42]

The abundance of expressed circRNAs in each sample were normalized as number of back-spliced reads per million mapped reads (BSRP), and a minimum BSRP cutoff was set to 0.1 for all samples. The number of circRNAs expressed at various cutoff expression levels in each sample are shown in Figure 1E and F. A total of 3,036 circRNAs were defined as highly expressed circRNA (BSRP > 1), and 2,579 of them were detected in the three developmental stages we examined (Fig. 1G). The 10 most abundant circRNAs expressed in embryonic muscle are listed in Table 1. The majority of highly expressed circRNAs was derived from exons and as a group was more abundant than other circRNA types (Fig. 1H). Our RNA sequencing data indicating circRNAs are also abundant in chicken embryonic muscle.

3.2. Identification of differentially expressed circRNAs

CircRNAs are usually expressed in tissue and developmental stage specific manners. Especially during embryonic development, circRNA expression levels exhibit dynamic global changes.[17,42,46] To address the potential functions of circRNA, differentially-expressed circRNAs (DEcircRNAs) were identified by DEGseq analysis (fold change > 2, q-value < 0.05) and clustered based on their expression profiles (Fig. 2A and Supplementary Fig. S4). A total of 462 DEcircRNAs were detected in the three developmental groups, 236, 285 and 89 circRNAs in E11_VS_E16, E11_VS_P1, and E16_VS_P1 comparison groups, respectively. These circRNAs were more abundant in E16 and P1 than in E11, whereas a small fraction of group E11 was quantitatively higher (Fig. 2B, Supplementary Tables S4–S6). We found that 223, 526 and 255 circRNAs were specifically expressed in E11, E16 and P1, respectively (Fig. 2C). A larger number of circRNAs are differentially expressed in chicken leg muscle development. We performed RNA sequencing used two individuals in each stage but not mix RNA pool. The variation of circRNAs abundance was also existed between the two duplicates used for sequencing. The numbers of circRNAs were larger in E16 or P1 than that in E11 of leg muscle, consistent with that circRNAs were found to accumulate during aging in Drosophila heads.[17]

The biogenesis of circRNA can competes with pre-mRNA splicing, and intron or exon-intron circRNAs can regulate the transcription of their parental gene.[23–25] In this study, we performed GO Enrichment Analysis for the parental genes of differentially-expressed circRNAs (fold change > 2, *P*-value < 0.05) in E11_VS_E16, E11_VS_P1 and E16_VS_P1 comparison groups (Supplementary Tables S7–S9). The parental gene functions were involved in muscle-related biological processes, including muscle structure development, muscle tissue development, muscle system processes and muscle cell differentiation (Fig. 2D–F). Using this data, we organized a functional network using Ingenuity pathway analysis (Supplementary Table S10). The most prevalent diseases and function interaction network was related to skeletal and muscular disorders and this group involved 29 parental genes (Supplementary Fig. S5).

3.3. Putative functions of chicken circRNAs as miRNA sponges

The spatial-temporal grouping of circRNAs suggested that they are functional molecules. Since the discovery of *CDR1as* can serve as

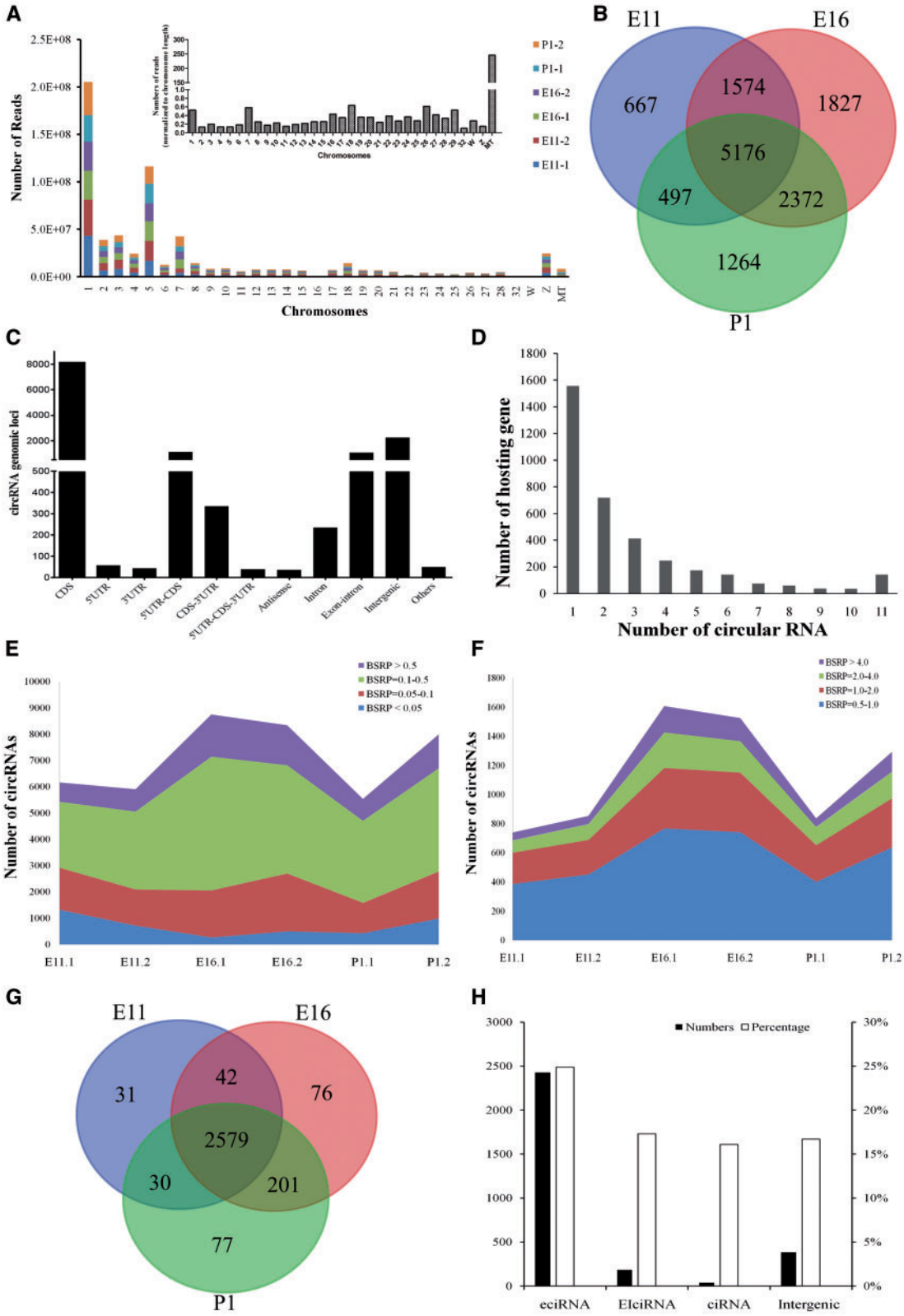

Figure 1. Annotation of chicken embryonic muscle circRNA. (A) Distribution of sequencing reads on chicken chromosome. (B) Venn diagrams of circRNAs in embryonic muscle with three different development stages. E11, 11 embryo age; E16, 16 embryo age; P1, 1 day post hatch. (C) Genomic origin of chicken circRNA. (D) Distribution of circRNAs among genes; 11,064 circRNAs in 3,589 genes. (E, F) The number of circRNAs expressed at various cutoff expression levels. (G) Venn diagrams of highly expressed circRNAs ($n = 3{,}036$, BSRP > 1). (H) Numbers and percentages of different types of highly expressed circRNAs. The *Y* axis (left) represents the numbers of highly expressed circRNAs, and the *Y* axis (right) represents the percentage is the number of abundant circRNAs of type divided by the total number of circRNAs specific type. eciRNA, exonic circRNA; ElciRNA, exon-intron circRNA; ciRNA, intronic circRNA.

Table 1. The top 10 circRNAs expressed in chicken embryonic muscle

circRNA_ID	circRNA_type	Parental gene	Junction	Linear distance of junction (nt)	Length (nt)	BSRP
1:106020993|106024456	eciRNA	MORC3	Exon 5-7	3,464	428	328.06
5:24409706|24411456	eciRNA	MAPKBP1	Exon 25-27	1,751	396	279.82
2:14642365|14648660	EIciRNA	SVIL	Exon6-intron11(P)	6,296	6296	271.62
2:14633486|14648660	eciRNA	SVIL	Exon 6-14	15,174	1594	268.80
2:14645249|14648660	eciRNA	SVIL	Exon 6-10	3,412	504	179.63
7:14755660|14757838	eciRNA	MYPN	Exon 100-104	2,179	501	154.00
1:51782860|51783084	eciRNA	RBFOX2	Exon 2	2,25	225	134.95
4:1285647|1289769	eciRNA	FNDC3A	Exon 5-9	4,123	695	126.41
26:5104947|5107131	eciRNA	TAF8	Exon 2-5	2,185	444	120.12
1:51819796|51833118	eciRNA	RBFOX2	Exon 9-11	13,323	262	106.49

The expressed abundances of circRNAs were normalized as number of back-spliced reads per million mapped reads (BSRP). This column represented the sum of the BSRP values for all samples. eciRNA, exonic circRNA; EIciRNA, exon-intron circRNA.

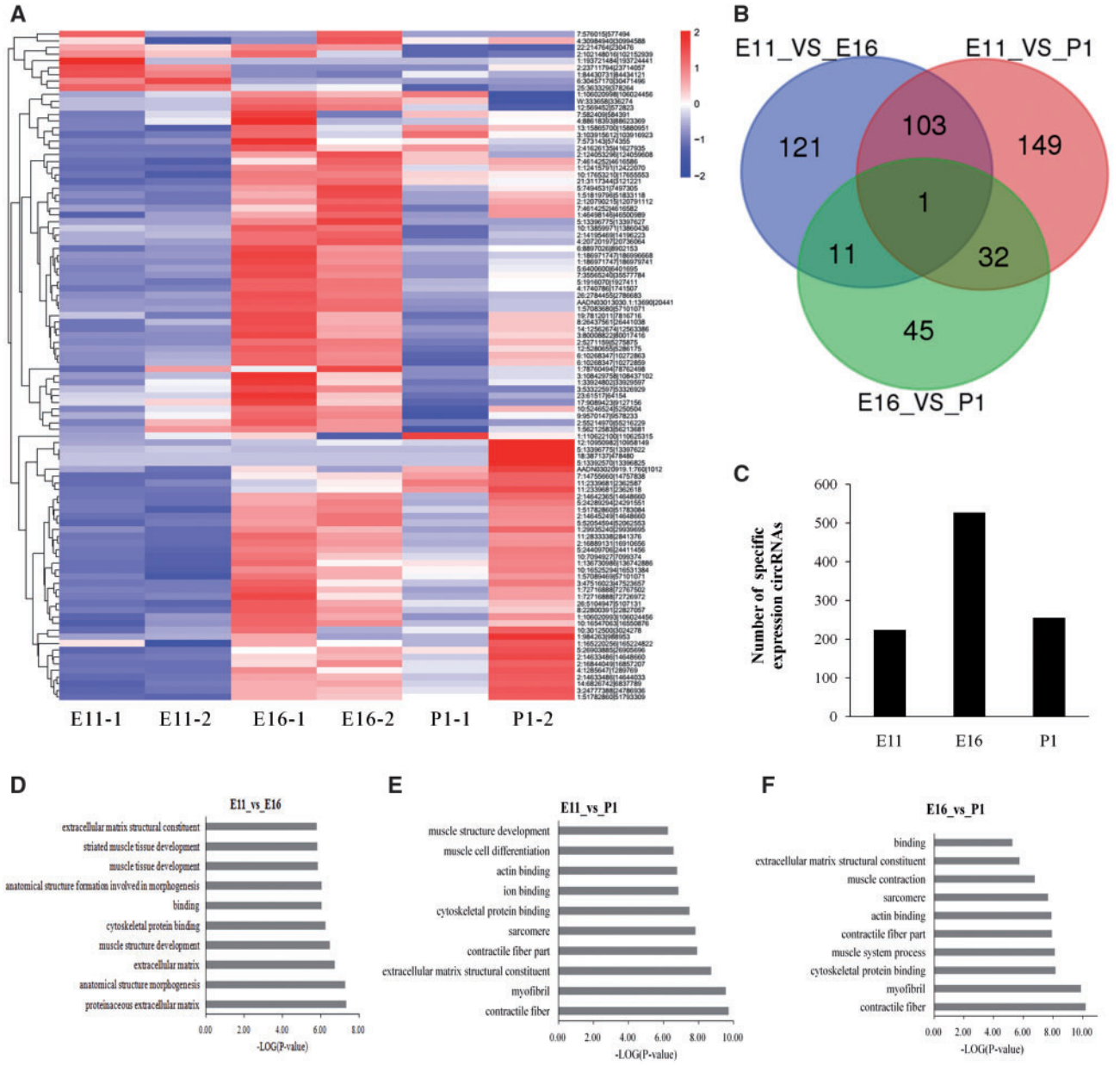

Figure 2. Differentially expressed circRNAs in three different development stages of embryonic muscle. (A) Heatmap of top 100 differentially expressed circRNAs in E11, E16 and P1 of leg muscle. (B) Venn diagrams of differentially expressed circRNAs ($n = 462$; q value < 0.05, fold change > 2). (C) The circRNA specific expression in three different development stages of embryonic muscle. The top 10 GO enrichment term for the parental genes of differentially expressed circRNAs in E11_VS_E16 (D), E11_VS_P1 (E) and E16_VS_P1 (F). The *Y* axis represents GO terms and the *X* axis represents –Log *p*-value.

Table 2. The top 10 differentially expressed eciRNAs with miRNA binding sites

circRNA_ID	E11_base Mean	E16_base Mean	P1_base Mean	Parental gene	Junction	Length (nt)	Target miRNAs
2:14633486|14648660	313.35	5345.71	7148.93	SVIL	Exon6-14	1594	miR-31-5p (2), miR-103-3p (2), miR-135a-5p (2), miR-203a, miR-1720-3p, miR-1737
7:14755660|14757838	14.79	2547.25	5155.27	TNN	Exon100-104	501	miR-133a-5p, miR-1a-2-5p, miR-22-5, miR-451
26:5104947|5107131	561.47	2995.87	2333.66	TAF8	Exon2-5	444	miR-34a-5p
1:51819796|51833118	626.95	2756.90	1891.00	RBFOX2	Exon9-11	262	miR-18b-3p
2:14633486|14644033	354.24	1777.35	1973.62	SVIL	Exon11-14	1090	miR-31-5p, miR-103-3p (2), miR-135a-5p (2), miR-1720-3p
5:13396775|13397627	0.00	3666.12	0.00	TNNT3	Exon15-17	297	miR-6631-5p
1:84430731|84434121	1992.44	171.80	690.86	ABI3BP	Exon31-34	273	miR-499-3p (2)
6:30457170|30471496	2015.87	101.28	47.48	FGFR2	Exon3-6	636	miR-15a, miR-200a-3p
1:51782860|51793309	165.19	775.20	1025.64	RBFOX2	Exon2-3	372	miR-1a-3p, miR-206
7:35565240|35577784	246.91	912.57	451.10	GPD2	Exon1-5	667	miR-103-3p (2), miR-133a-3p, miR-133b, miR-133c-3p, miR-30a-5p

Read counts of each sample were normalized by DESEQ software. Base Mean is the average normalized value of two samples at same time point. The numbers in brackets are target sites for each miRNA.

miR-7 sponges,[13,14] there are growing evidences indicate that circRNAs can function as miRNA sponges or competing endogenous RNAs.[17,47–51] However, unlike *CDR1as* contain multiple binding sites to sponge miR-7, most circRNAs bind more than one species of miRNA as was shown for *circFOXO3*[52] and *circHIPK3*.[53] We identified the miRNA binding capabilities of our differentially expressed exonic circRNAs, and found that 946 of 1,401 exonic circRNAs harbored one or more miRNA binding site and involved 150 known miRNAs (The top 10 of these circRNAs were listed in Table 2). We used the 20 most abundant differentially expressed exonic circRNAs from each comparison group and matched them with their potential target miRNAs. These data were then used to construct an interactive network map (Fig. 3). We identified several miRNAs with key roles in skeletal muscle development and differentiation such as miR-1, miR-133, miR-206 and miR-203 in this network. The high abundance of these DEcircRNAs could be served as candidate circRNAs to further study in chicken skeletal muscle.

The miR-1 and miR-206 are well-studied muscle-specific miRNAs that are necessary for skeletal muscle development as well as proliferation and differentiation of muscle cells.[52,53] Interestingly, we found that circRNA derived from the *RBFOX2* gene harbored binding sites for gga-miR-1a-3p and gga-miR-206. We identified 11 isoforms of *RBFOX2* circRNAs (Fig. 4A) and six of them were expressed abundantly and differentially in muscle (Fig. 4B). Four isoforms *circRBFOX2.2-3*, *2-4*, *2-6*, and *2-9* harbored miR-1a-3p and miR-206 binding sites (Fig. 4C). The interaction of circRBFOX2s with miR-1a-3p and miR-206 was further validated in our study.

3.4. Experimental validation of chicken circRNAs

The expression and back-splicing sites of several circRNAs were validated by divergent reverse-transcription PCR, RNaseR digestion and qRT-PCR, according to previously described methodologies.[13,54] Divergent primers and convergent primers were designed to amplify six candidate circRNAs in cDNA and genomic DNA samples. Divergent primers from each circRNA produced a single distinct band of the expected product size only in cDNA samples suggesting the presence of back-splicing junctions but not genomic rearrangements (Fig. 5A). PCR products of divergent primers were further detected by Sanger sequencing to confirm the back-splicing junctions (Fig. 5B and Supplementary Fig. S6). To detect the resistance of circRNA to the digestion by RNaseR, we quantified the six candidate circRNAs with RNaseR treatment compared to control by qRT-PCR. All tested circRNAs showed much more resistant than the linear mRNA control (Fig. 5C). In addition, the expression of six differentially expressed circRNAs was also validated by qRT-PCR in E11_VS_E16, E11_VS_P1, and E16_VS_P1 comparison groups. Except the expression of *circRBFOX2.2-4* and *circFGFR2.3-6* in P1 VS E16 compared group, the expression patterns of these circRNAs were consistent with the RNA-Seq results, indicating that the deep sequencing results were reliable (Fig. 5D).

3.5. CircRBFOX2 interacts with miR-206 and miR-1a

Two circular isoforms of *RBFOX2* which we designated as *circRBFOX2.2-3* and *circRBFOX2.2-4* were derived from exon2-3 and exon 2-4 of *RBFOX2*, respectively. Both these molecules possessed miR-1a-3p and miR-206 binding sites (Fig. 6A and B). The prediction of a miRNA target site does not necessarily mean that a miRNA binds to that site. To further validate that these two circRBFOX2s can be interacted with miR-1a-3p and miR-206, we constructed two dual-luciferase reporters by inserting perfect miR-1a-3p or miR-206 target sites into the 3' end of *Renilla* luciferase. The knockdown potential of the miRNA was assessed by the presence or absence of circRBFOX2s. After co-transfecting the dual-luciferase reporter with their corresponding miRNAs, the relative luminescence was significantly decreased compared with miR-NC. However, the relative luminescence returned when co-transfected with either *circRBFOX2.2-3* or *circRBFOX2.2-4* expression vectors, but not the mutated vectors of circRBFOX2s (Fig. 6C and D). These results demonstrated that the knockdown potential of miR-1a-3p or miR-206 was significantly diminished in the presence of *circRBFOX2.2-3* and *circRBFOX2.2-4*. Immunoprecipitation of AGO2 from myoblasts co-transfected with miR-1a-3p, miR-206 or miR-203 and circRBFOX2 overexpression vector was performed and the circRNA levels were quantified by qRT–PCR and normalized to *GAPDH* (Fig. 6A). Compared with miR-203 transfected cells, immunoprecipitation of AGO2 from miR-1a-3p or miR-206 transfected cells were both resulted in an enrichment of circRBFOX2. In addition, compared with

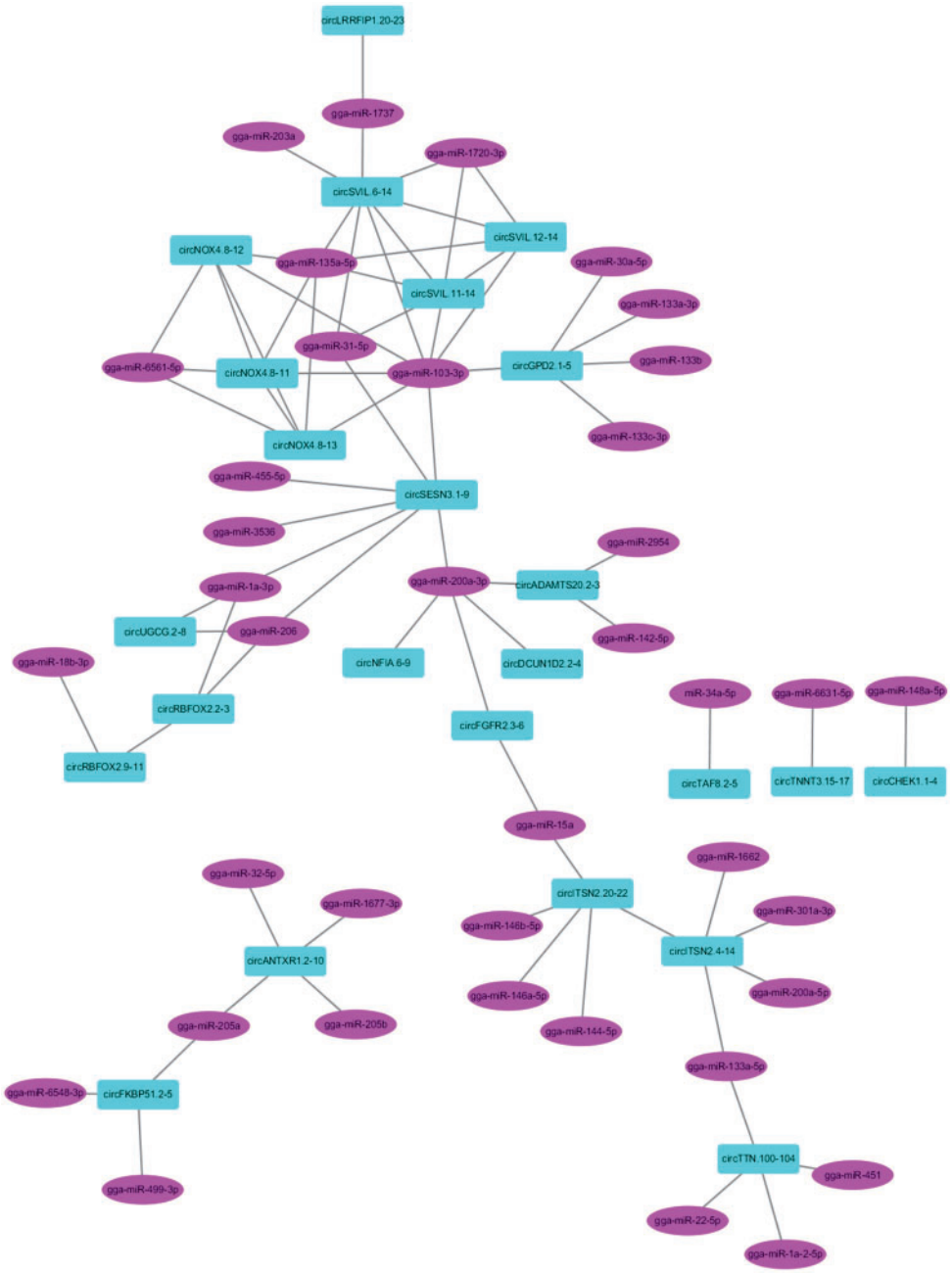

Figure 3. Interaction network of eciRNA and their potential target miRNAs. The top 20 differentially expressed exonic circRNAs of each comparison group and their potential target miRNAs were used for their interaction network analysis. Rectangle nodes represent circRNAs and circle nodes represent miRNAs.

miR-203 control, *circRBFOX2.2-4* was specifically captured by both 3-biotinylated miR-1a-3p and miR-206, and *circRBFOX2.2-3* was also captured by 3-biotinylated miR-206. Together, these results suggested that circRBFOX2s are able to interact with miR-1a-3p and miR-206.

3.6. Effects of circRBFOX2 on expression of miRNAs and their target genes

We over expressed or knocked down *circRBFOX2.2-3* and *circRBFOX2.2-4* in chicken primary myoblast, and then measured miR-1°-3p and miR-206 expression levels by qRT-PCR. We constructed the pcDNA3.1 vector with linear exon2-3 or exon2-4 of RBFOX2 as control, which give rise to linear RBFOX2 products. We transfected these linear control vector in myoblast and then the miR-206/miR-1a-3p level were quantified by qRT-PCR. The results showed that linear RBFOX2 did not affect the expression of miR-206 and miR-1a-3p (Fig. 7A).

Compared to empty vector control, overexpressed *circRBFOX2.2-3* or *circRBFOX2.2-4* inhibited both miR-1a-3p and miR-206, while the mutation of *circRBFOX2* vector did not have significant change (Fig. 7B). Furthermore, the expression level of miR-206/miR-1a-3p tend to be lower when the level of circRBFOX2s higher (Fig. 7C). We knock down *circRBFOX2.2-3*

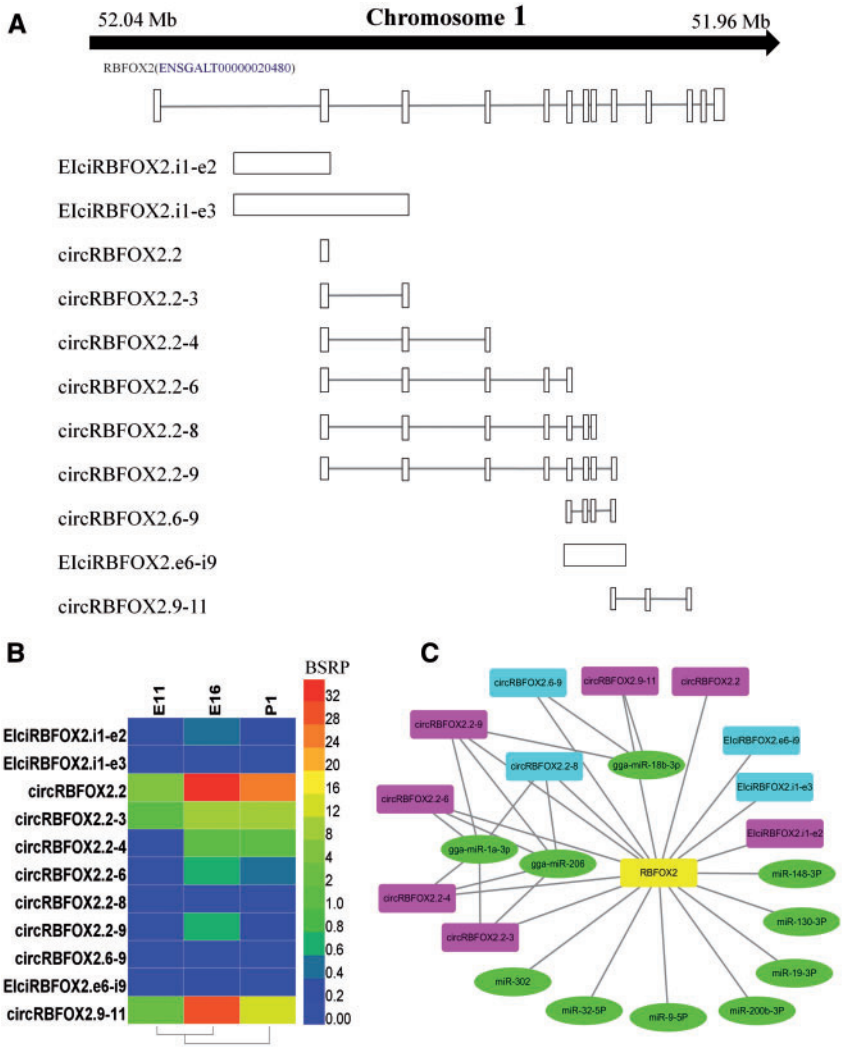

Figure 4. Annotation of circular RBFOX2 gene. (A) All circRNA isoforms of the RBFOX2 gene in chicken embryonic muscle. (B) The abundance of circular RBFOX2 in chicken embryonic muscle. The scale bar 0–32 represents the abundance of circRNAs (BSRP value). (C) Network of circular *RBFOX2* with miRNAs. Dark gray rectangle nodes represent highly-expressed circRNAs, light gray rectangle nodes represent low expressed circRNAs and circle nodes represent miRNAs.

and *circRBFOX2.2-4* using siRNAs, and the results showed that the siRNAs could knockdown the circRBFOX2s but not linear RBFOX2. Knockdown of either *circRBFOX2.2-3* or *circRBFOX2.2-4* increased both the expression of miR-1a-3p and miR-206 (Fig. 7D). Northern blot analysis for miR-206 was also confirmed that the miR-206 expression level was increased by knockdown of circRBFOX2s (Fig. 7H). The expression of miR-203 used as control did not affect by neither overexpressed nor knockdown of circRBFOX2s. Together, our results found that circRBFOX2s downregulated the expression of miR-1a-3p and miR-206. This finding was not consisted with the standard model of circRNA miRNA sponge. The circRNAs that act as miRNA sponge can sequesters the miRNA away from other targets, but does not necessarily alter the expression of the miRNA. Recently, there are some circRNAs, such as *CircRar1*, *circ-ABCB10* and hsa-circ-0016347 were also reported to downregulated the expression of their target miRNA.[55–57] However, the exact mechanism for this association is unknown, probably upregulation of circRNAs might degrade miRNA expression.

We further validated whether *circRBFOX2.2-3* and *circRBFOX2.2-4* regulated the target gene of miR-206. According to previous studies and predicted by Targetsclan (http://www.targetscan.org/vert_71/ (16 September 2017, date last accessed)), we chose the CCND1, CCND2, PAX3 and HDAC4 as candidate target gene for miR-206, and then verified their relations by luciferase assay.[58–60] The CCND2 and HDAC4 were confirmed as the target gene of miR-206 (Fig. 7A). Thus, we further determine their expression level after overexpression/knockdown of circRBFOX2s in myoblast. The results showed that both circRBFOX2.2-3 and circRBFOX2.2-4 upregulated the mRNA level of CCND2 but not HDAC4 (Fig. 7F and G).

3.7. Effects of circRBFOX2 and miR-206 on myoblast proliferation

To observe the functions of *circRBFOX2.2-3* or *circRBFOX2.2-4* on myoblast, we over expressed and knocked down the *circRBFOX2.2-3* or *circRBFOX2.2-4* by transfected with overexpression vector or siRNAs. Overexpression of either *circRBFOX2.2-3* or *circRBFOX2.2-*

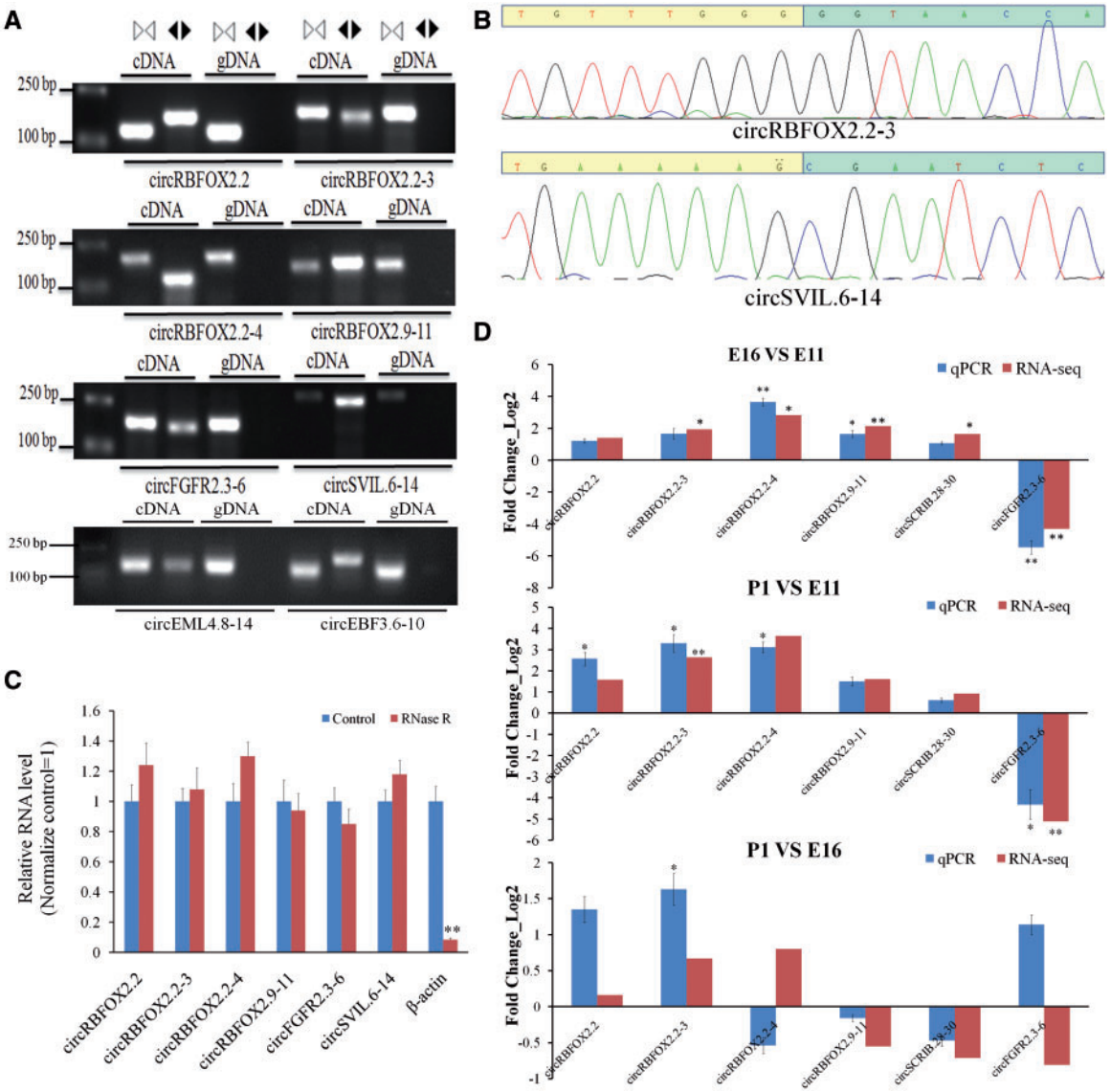

Figure 5. Experimental validation of circular RNAs. (A) Divergent primers amplify circRNAs in cDNA but not genomic DNA (gDNA). White triangles represent convergent primers and black triangles represent divergent primers. (B) Sanger sequencing confirmed the back-splicing junction sequence of circRNAs. (C) qRT-PCR showing resistance of circRNAs to RNaseR digestion. (D) qRT-PCR validation of six differentially expressed circRNAs in all three comparisons. qRT-PCR reactions were run in triplicate and presented as means ± S.E.M. The Student's t-test was used to compare expression levels among different groups. $*P < 0.05$; $**P < 0.01$.

4 resulted in increased levels of *circRBFOX2.2-3* or *circRBFOX2.2-4* above that of the empty vector control (Fig. 8A and B). Similarly, when we transfected *circRBFOX2.2-3* or *circRBFOX2.2-4* siRNAs, the transcript levels of both these RNAs decreased (Fig. 8C and D). These results indicated that our expression system worked in myoblasts. We used flow cytometry for cell cycle analysis of transfected myoblasts. Overexpression of *circRBFOX2.2-3* resulted in a greater number of S-phase cells than controls, and fewer G0/G1 cells (Fig. 8E and F, Supplementary Figs S7 and S8). Both the mutated vector of *circRBFOX2.2-3* and *circRBFOX2.2-4* did not affect the cell cycle of myoblast. Knockdown of *circRBFOX2.2-3* resulted in a greater number of G0/G1 cells and fewer S and G2/M phase cells than controls. However, the *circRBFOX2.2-4* knockdown and overexpression groups showed significant differences only in S-phase (Fig. 8E and F, Supplementary Figs S7 and S8). The 5-Ethynyl-2'-deoxyuridine (EdU) incorporation assays were also performed after over expressed and knocked down the *circRBFOX2.2-3* or *circRBFOX2.2-4* in myoblast. The number of EdU-stained cells increased in both the *circRBFOX2.2-3* and *circRBFOX2.2-4* overexpression groups. In contrast, proliferation decreased when *circRBFOX2.2-3* and *circRBFOX2.2-4* were knocked down (Fig. 8G and H).

Muscle-specific miR-206 has been reported to inhibit cell proliferation in human and mouse.[58–59] The effects of miR-206 in myoblast proliferation were also examined using cell cycle and EdU incorporation analysis. We overexpressed and knocked down miR-206 by transfecting myoblasts with a miR-206 mimic or anti-miR-206 (Fig. 9A and B). Myoblasts transfected with the miR-206 mimic decreased the number of S-phase cells compared with the scrambled negative control group (Fig. 9C). Conversely, S-phase cells in the anti-miR-206 group were significantly increased (Fig. 9D). Consistent with the result

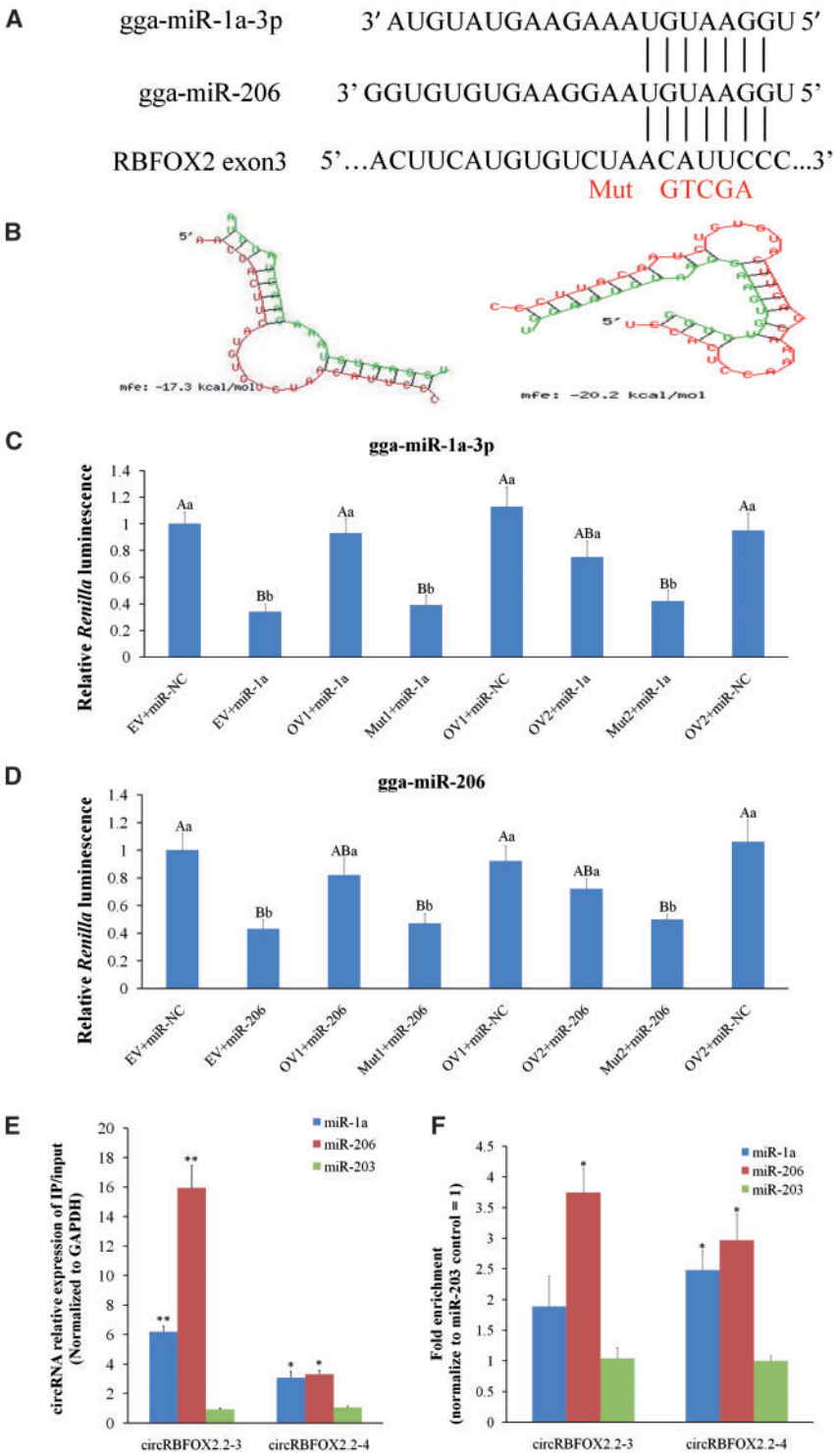

Figure 6. CircRBFOX2s interacted with miR-206 and miR-1a-3p. (A) The predicted binding site of miR-1a-3p and miR-206 in the exon3 of RBFOXO2. Mut indicates the mutation sequences of binding sites. (B) miR-1a-3p and miR-206 targeting site in circRBFOX2s analysed by RNAhybrid software. Luciferase reporter assays for miR-1a-3p (C) and miR-206 (D). Luminescence was measured 48 h after transfected with the luciferase reporter and miRNA mimics or NC (negative control) and with circRNAs overexpression vector, circRNA mutated vector or empty vector. The relative levels of *Renilla* luminescence normalized to firefly luminescence are plotted. Error bars represent S.D. ($n = 6$). OV1, overexpression vector of *circRBFOX2.2-3*; OV2, overexpression vector of *circRBFOX2.2-4*; Mut1, mutated vector of circRBFOX2.2-3; Mut2, mutated vector of *circRBFOX2.2-4*; EV, empty vector. (E) Immunoprecipitation of AGO2 from myoblasts co-transfected with miR-1a-3p, miR-206 or miR-203 and circRBFOX2 overexpression vector. The circRNA levels were quantified by qRT–PCR and normalized to the GAPDH, the fold change of immunoprecipitate/input are plotted. Error bars represent S.D. ($n = 3$). (F) qRT–PCR analysis of circRBFOX2s level in the streptavidin captured fractions from the myoblast lysates after transfection with 3-end biotinylated miR-1a-3p, miR-206 or miR-203 control. Error bars represent S.D. ($n = 3$). Student's t test (two-tailed) was performed for data analysis. $^{*}P < 0.05$; $^{**}P < 0.01$.

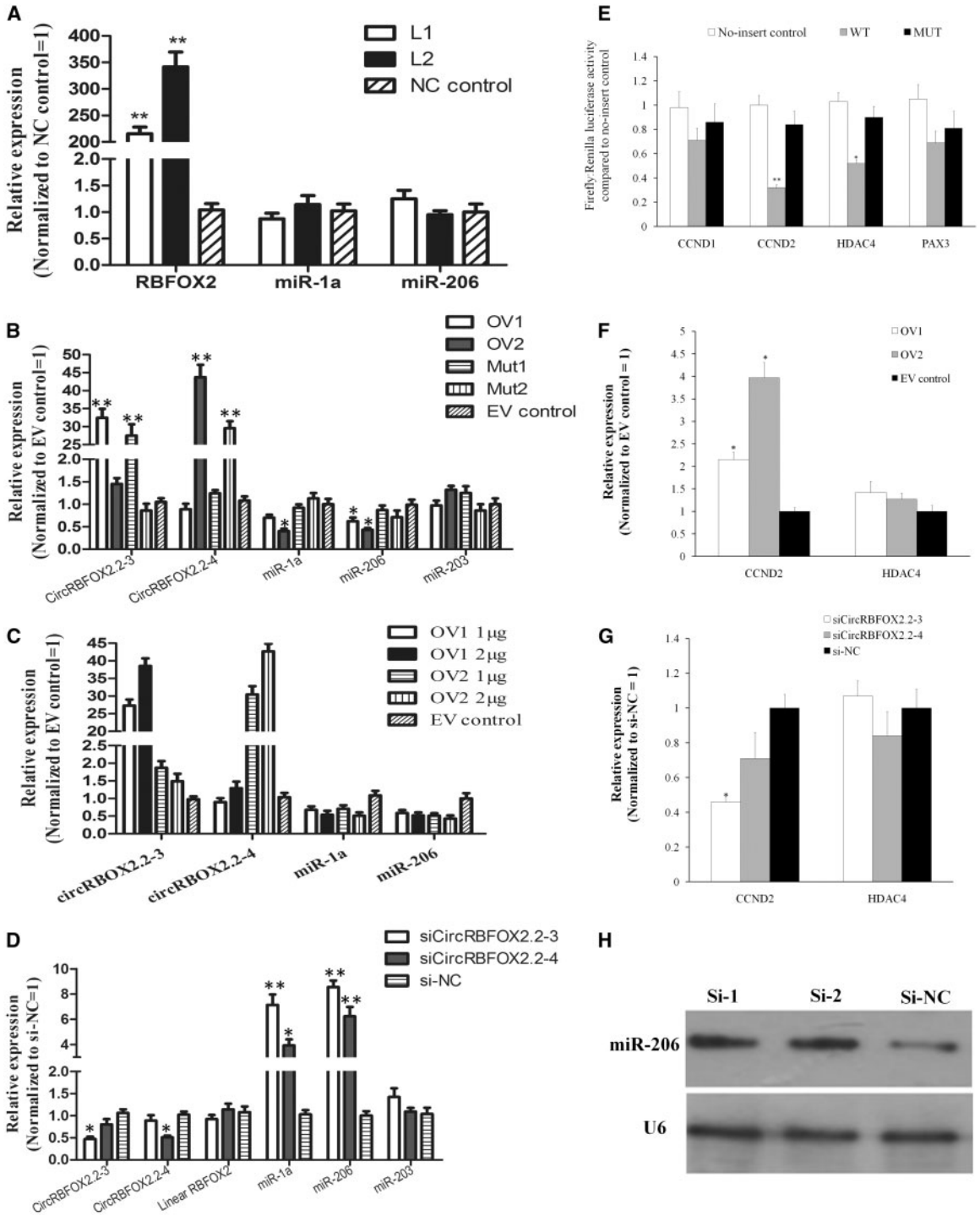

Figure 7. Effects of circRBFOX2 on expression of miRNAs and their target gene. (A) Linear *RBFOX2* did not affect the expression of miR-206 and miR-1a-3p. The miR-206 and miR-1a-3p level were quantified by qRT-PCR after transfected with linear *RBFOX2* overexpression vector or pcDNA3.1 empty vector. L1 represents linear exon2-3 of *RBFOX2* overexpression vector; L2 represents linear exon2-4 of *RBFOX2* overexpression vector; NC control represents pcDNA3.1 empty vector. (B) Overexpression of *circRBFOX2.2-3* or *circRBFOX2.2-4* inhibits miR-1a-3p and miR-206 expression. The expression level of miR-1a-3p, miR-206 and miR-203 control was detected after transfected with circRNAs overexpression vector, circRNA mutated vector or empty vector. Bars represent S.D. ($n = 4$). (C) The effects different fold change of *circRBFOX2.2-3* or *circRBFOX2.2-4* on miR-1a-3p and miR-206 expression. (D) Knockdown of *circRBFOX2.2-3* or *circRBFOX2.2-4* increases miR-1a-3p and miR-206 abundance. The expression level of miR-1a-3p, miR-206 and miR-203 control was detected after transfected with siRNA of circRBFOX2 or si-NC. Bars represent S.D. ($n = 4$). (E) Luciferase assay for miR-206 and their target genes. The relative luminescence was measured 48 h after co-transfected with miR-206 mimic and luciferase reporters of no-insert control, wide type target sequence of target genes (WT) or mutated target sequence of target genes (MUT) in DF-1 cell. Error bars represent S.D. ($n = 4$). The relative levels of *CCND2* and *HDAC4* were quantified by qRT–PCR after overexpressed (F) or knockdown (G) of *circRBFOX2.2-3* or *circRBFOX2.2-4* in chicken myoblast. Error bars represent S.D. ($n = 4$). (H) Knockdown of *circRBFOX2.2-3* or *circRBFOX2.2-4* increases the expression of miR-206. The expression level of miR-206 was detected after transfected with siRNA of circRBFOX2 or si-NC by Northern blotting. OV1, overexpression vector of *circRBFOX2.2-3*; OV2, overexpression vector of circRBFOX2.2-4; Mut1, mutated vector of *circRBFOX2.2-3*; Mut2, mutated vector of circRBFOX2.2-4; EV, empty vector; Si-1, siRNA of *circRBFOX2.2-3*; Si-2, siRNA of *circRBFOX2.2-4*; Si-NC, negative control. Student's *t* test (two-tailed) was performed for data analysis. $^*P < 0.05$; $^{**}P < 0.01$.

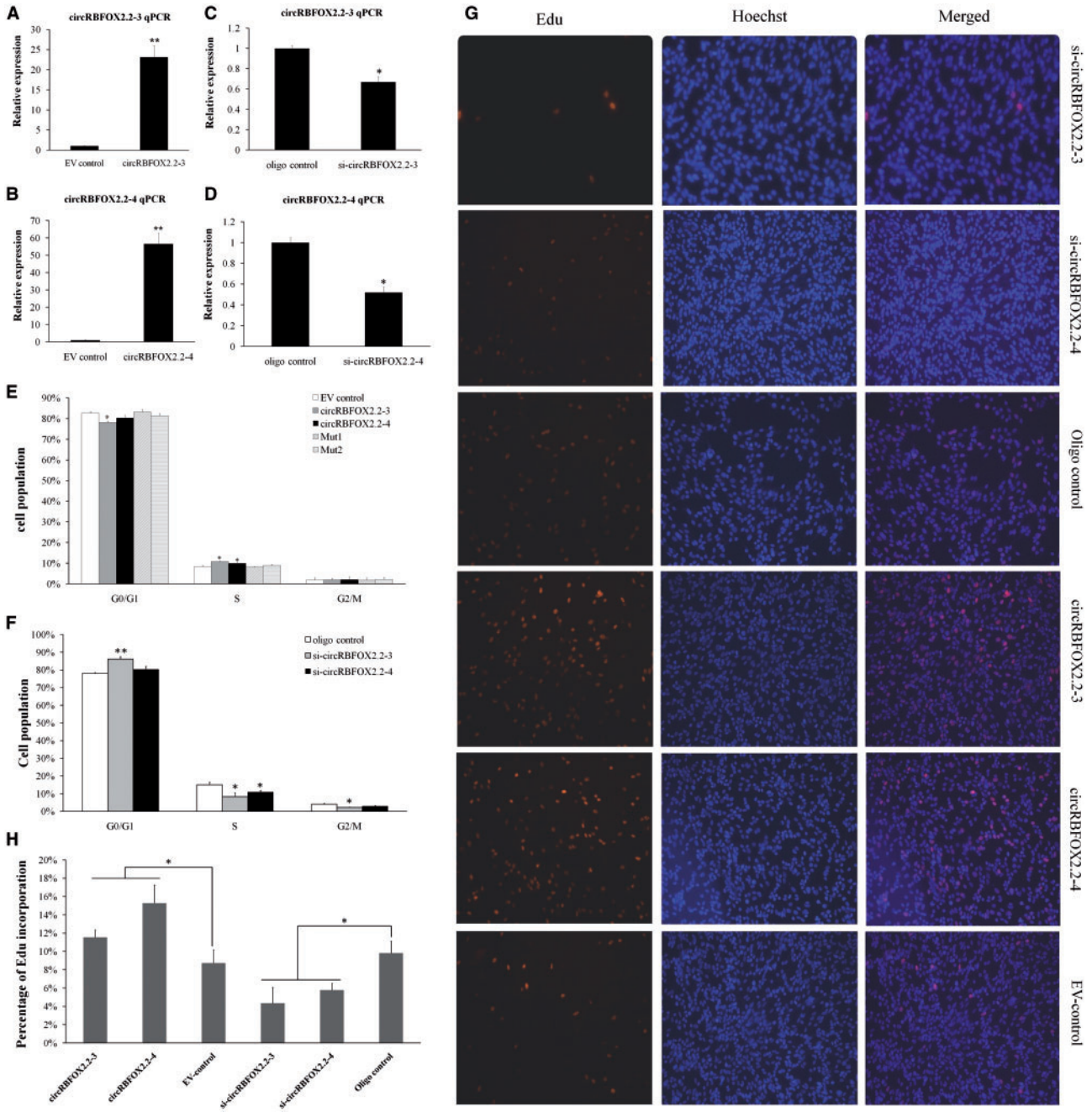

Figure 8. Chicken circRBFOX2.2-3 and circRBFOX2.2-4 regulate QM-7 cell proliferation. Overexpression of *circRBFOX2.2-3* (A) and *circRBFOX2.2-4* (B). The relative expression was determined by qRT-PCR in QM-7 after transfected with overexpression vector or EV control. Knocked down of *circRBFOX2.2-3* (C) and *circRBFOX2.2-4* (D). The relative expression was determined by qRT-PCR in QM-7 after transfected with si-circRBFOX2.2-3, si-circRBFOX2.2-4 or oligo control. Cell cycle analysis of myoblasts transfected with (E) overexpression vectors, mutated vector or (F) siRNAs were performed using propidium iodide staining for DNA content and a FACSAriaII flow cytometer. Bars represent S.D. ($n = 4$). OV1, overexpression vector of *circRBFOX2.2-3*; OV2, overexpression vector of *circRBFOX2.2-4*; Mut1, mutated vector of *circRBFOX2.2-3*; Mut2, mutated vector of *circRBFOX2.2-4*; EV, empty vector. (G) Photomicrographs of QM-7 myoblasts stained with EdU to assess proliferation. Cells were transfected with either overexpression vectors or siRNAs and assayed after 48 h. EdU (red) fluorescence indicates proliferation. Nuclei are indicated by Hoechst (blue) fluorescence. All photomicrographs are at 200× magnification. (H) The percentage of EdU-stained cells per total cell numbers. Error bars represent S.D. ($n = 3$). Student's t test (two-tailed) was performed for data analysis. $^{*}P < 0.05$; $^{**}P < 0.01$.

of cell cycle analysis, EdU incorporation indicated that myoblast proliferation was suppressed by miR-206 overexpression and increased by miR-206 knockdown (Fig. 9A and F). Interestingly, the effects of miR-206 on myoblast proliferation was impaired when either *circRBFOX2.2-3* or *circRBFOX2.2-4* vectors were co-transfected (Fig. 9E and F). Together, these data implied that miR-206 could suppress myoblast proliferation, whereas *circRBFOX2.2-3* and *circRBFOX2.2-4* can promote myoblast proliferation, and antagonize the functions of miR-206 in myoblasts. Our results support previous findings that circRNAs sequester miRNAs to suppress their functions in chickens. Nevertheless, only a few circRNAs that function in this manner have been described. Some reports argue that most circRNAs

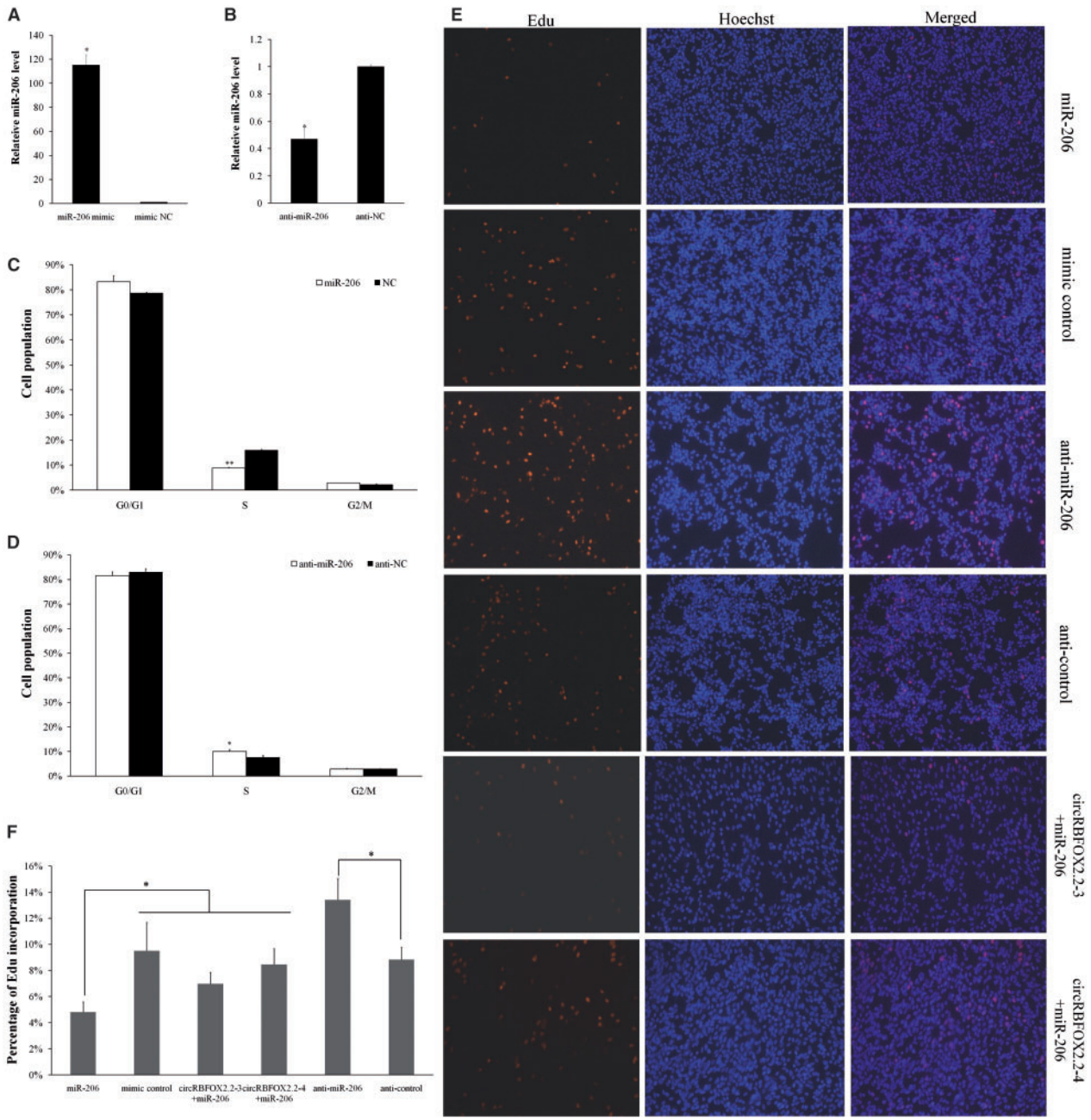

Figure 9. The effect of miR-206 on QM-7 cell proliferation was rescued by circRBFOX2s. (A) miR-206 expression was determined by qRT-PCR in QM-7 cells after transfection with a miR-206 mimic or control duplexes. (B) miR-206 expression was determined by qRT-PCR in QM-7 cells after transfection with anti-miR-206 or anti-NC. Cell cycle analysis of myoblasts transfected with miR-206 mimic (C) or anti-miR-206 (D) using propidium iodide staining for DNA content and a FACSAriall flow cytometer. Bars represent S.D. ($n = 4$). $^*P < 0.05$; $^{**}P < 0.01$. (E) EdU assays were performed in QM-7cells after 48 h co-transfected a miR-206 mimic, mimic control, anti-miR-206, anti-NC, miR-206 mimic with *circRBFOX2.2-3* or *circRBFOX2.2-4* overexpression vector. Cells were fluorescently stained with EdU (red). Nuclei were stained with Hoechst (blue). All photomicrographs are at 200 × magnification. (F) The percentage of EdU-stained cells per total number. Error bars represent S.D. ($n = 3$); $^*P < 0.05$.

do not function as miRNA sponges in human and mouse.[20,61,62] Whether this mechanism is a common theme in circRNA biology awaits future research.

In summary, we performed genome-wide identification of chicken circRNAs by RNA sequencing, and found they are abundant and differentially expressed during chicken embryonic development. Most of the exonic circRNAs harbored miRNA binding sites and could play key roles in embryonic muscle development through sequestering miRNAs as well as other functions.

Acknowledgements

We thank Prof. Zhang's lab members for helpful discussions and the SCAU chicken farm for providing breeding eggs.

Accession numbers

RNA-seq data are available in the Gene Expression Omnibus (GEO) with accession number (GSE89355).

Supplementary data

Supplementary data are available at *DNARES* online.

Funding

This research was supported by the Natural Scientific Foundation of China (31472090), the China Agriculture Research System (CARS-41-G03), and the Foundation for High-level Talents in Higher Education in Guangdong, China.

Conflict of interest

None declared.

References

1. Djebali, S., Davis, C. A., Merkel, A., et al. 2012, Landscape of transcription in human cells, *Nature*, **489**, 101–8.
2. Batista, P. J., and Chang, H. Y. 2013, Long noncoding RNAs: cellular address codes in development and disease, *Cell*, **152**, 1298–307.
3. Bartel, D. P. 2009, MicroRNAs: target recognition and regulatory functions, *Cell*, **136**, 215–33.
4. Ponting, C. P., Oliver, P. L., and Reik, W. 2009, Evolution and functions of long noncoding RNAs, *Cell*, **136**, 629–41.
5. Guttman, M., and Rinn, J. L. 2012, Modular regulatory principles of large non-coding RNAs, *Nature*, **482**, 339–46.
6. Sanger, H. L., Klotz, G., Riesner, D., Gross, H. J., and Kleinschmidt, A. K. 1976, Viroids are single-stranded covalently closed circular RNA molecules existing as highly base-paired rod-like structures, *Proc. Natl Acad. Sci. USA*, **73**, 3852–6.
7. Capel, B., Swain, A., Nicolis, S., et al. 1993, Circular transcripts of the testis-determining gene Sry in adult mouse testis, *Cell*, **73**, 1019–30.
8. Zaphiropoulos, P. G. 1996, Circular RNAs from transcripts of the rat cytochrome P450 2C24 gene: correlation with exon skipping, *Proc Natl Acad. Sci. U S A*, **93**, 6536–41.
9. Zaphiropoulos, P. G. 1997, Exon skipping and circular RNA formation in transcripts of the human cytochrome P-450 2C18 gene in epidermis and of the rat androgen binding protein gene in testis, *Mol. Cell. Biol.*, **17**, 2985–93.
10. Li, X. F., and Lytton, J. 1999, A circularized sodium-calcium exchanger exon 2 transcript, *J. Biol. Chem.*, **274**, 8153–60.
11. Cocquerelle, C., Mascrez, B., Hetuin, D., and Bailleul, B. 1993, Mis-splicing yields circular RNA molecules, *FASEB J.*, **7**, 155–60.
12. Salzman, J., Chen, R. E., Olsen, M. N., Wang, P. L., and Brown, P. O. 2013, Cell-type specific features of circular RNA expression, *PLoS Genet.*, **9**, e1003777.
13. Memczak, S., Jens, M., Elefsinioti, A., et al. 2013, Circular RNAs are a large class of animal RNAs with regulatory potency, *Nature*, **495**, 333–8.
14. Hansen, T. B., Jensen, T. I., Clausen, B. H., et al. 2013, Natural RNA circles function as efficient microRNA sponges, *Nature*, **495**, 384–8.
15. Rybak-Wolf, A., Stottmeister, C., Glazar, P., et al. 2015, Circular RNAs in the mammalian brain are highly abundant, conserved, and dynamically expressed, *Mol. Cell*, **58**, 870–85.
16. Ivanov, A., Memczak, S., Wyler, E., et al. 2015, Analysis of intron sequences reveals hallmarks of circular RNA biogenesis in animals, *Cell Rep.*, **10**, 170–7.
17. Westholm, J. O., Miura, P., Olson, S., et al. 2014, Genome-wide analysis of drosophila circular RNAs reveals their structural and sequence properties and age-dependent neural accumulation, *Cell Rep.*, **9**, 1966–80.
18. Wang, P. L., Bao, Y., Yee, M. C., et al. 2014, Circular RNA is expressed across the eukaryotic tree of life, *PLoS One*, **9**, e90859.
19. Ye, C. Y., Chen, L., Liu, C., Zhu, Q. H., and Fan, L. 2015, Widespread noncoding circular RNAs in plants, *New Phytol.*, **208**, 88–95.
20. Guo, J. U., Agarwal, V., Guo, H., and Bartel, D. P. 2014, Expanded identification and characterization of mammalian circular RNAs, *Genome Biol.*, **15**, 409.
21. Salzman, J., Gawad, C., Wang, P. L., Lacayo, N., and Brown, P. O. 2012, Circular RNAs are the predominant transcript isoform from hundreds of human genes in diverse cell types, *PLoS One*, **7**, e30733.
22. Jeck, W. R., Sorrentino, J. A., Wang, K., et al. 2013, Circular RNAs are abundant, conserved, and associated with ALU repeats, *RNA*, **19**, 141–57.
23. Zhang, Y., Zhang, X. O., Chen, T., et al. 2013, Circular intronic long noncoding RNAs, *Mol. Cell*, **51**, 792–806.
24. Li, Z., Huang, C., Bao, C., et al. 2015, Exon-intron circular RNAs regulate transcription in the nucleus, *Nat. Struct. Mol. Biol.*, **22**, 256–64.
25. Ashwal-Fluss, R., Meyer, M., Pamudurti, N. R., et al. 2014, circRNA biogenesis competes with pre-mRNA splicing, *Mol. Cell*, **56**, 55–66.
26. Granados-Riveron, J. T., and Aquino-Jarquin, G. 2016, The complexity of the translation ability of circRNAs, *Biochim. Biophys. Acta*, **1859**, 1245–51.
27. Chen, X., Han, P., Zhou, T., Guo, X., Song, X., and Li, Y. 2016, circRNADb: A comprehensive database for human circular RNAs with protein-coding annotations, *Sci. Rep.*, **6**, 34985.
28. Yang, Y., Fan, X., Mao, M., et al. 2017, Extensive translation of circular RNAs driven by N6-methyladenosine, *Cell Res.*, **27**, 626–41.
29. Legnini, I., Di Timoteo, G., Rossi, F., et al. 2017, Circ-ZNF609 Is a Circular RNA that Can Be Translated and Functions in Myogenesis, *Mol. Cell*, **66**, 22–37.
30. Bassel-Duby, R., and Olson, E. N. 2006, Signaling pathways in skeletal muscle remodeling, *Annu. Rev. Biochem.*, **75**, 19–37.
31. Schiaffino, S., Sandri, M., and Murgia, M. 2007, Activity-dependent signaling pathways controlling muscle diversity and plasticity, *Physiology (Bethesda)*, **22**, 269–78.
32. Luo, W., Nie, Q., and Zhang, X. 2013, MicroRNAs involved in skeletal muscle differentiation, *J. Genet. Genomics*, **40**, 107–16.
33. Nie, M., Deng, Z. L., Liu, J., and Wang, D. Z. 2015, Noncoding RNAs, Emerging Regulators of Skeletal Muscle Development and Diseases, *Biomed. Res. Int.*, **2015**, 676575.
34. van Rossum, D., Verheijen, B. M., and Pasterkamp, R. J. 2016, Circular RNAs: Novel Regulators of Neuronal Development, *Front. Mol. Neurosci.*, **9**, 74.
35. Maiese, K. 2016, Disease onset and aging in the world of circular RNAs, *J. Transl. Sci.*, **2**, 327–9.
36. Qu, S., Zhong, Y., Shang, R., et al. 2016, The emerging landscape of circular RNA in life processes, *RNA Biol.*, 1–8.
37. Abdelmohsen, K., Panda, A. C., De S., et al. 2015, Circular RNAs in monkey muscle: age-dependent changes, *Aging (Albany NY)*, **7**, 903–10.
38. Fridolfsson, A., and Ellegren, H. 1999, A simple and universal method for molecular sexing of non-ratite birds, *J. Avian Biol.*, **30**, 116–21.
39. Trapnell, C., Pachter, L., and Salzberg, S. L. 2009, TopHat: discovering splice junctions with RNA-Seq, *Bioinformatics*, **25**, 1105–11.
40. Trapnell, C., Williams, B. A., Pertea, G., et al. 2010, Transcript assembly and quantification by RNA-Seq reveals unannotated transcripts and isoform switching during cell differentiation, *Nat. Biotechnol.*, **28**, 511–5.
41. Gao, Y., Wang, J., and Zhao, F. 2015, CIRI: an efficient and unbiased algorithm for de novo circular RNA identification, *Genome Biol.*, **16**, 4.
42. Veno, M. T., Hansen, T. B., Veno, S. T., et al. 2015, Spatio-temporal regulation of circular RNA expression during porcine embryonic brain development, *Genome Biol.*, **16**, 245.
43. Zhang, C., Wu, H., Wang, Y., et al. 2016, Circular RNA of cattle casein genes are highly expressed in bovine mammary gland, *J. Dairy Sci.*, **99**, 4750–60.
44. Halevy, O., Piestun, Y., Allouh, M. Z., et al. 2004, Pattern of Pax7 expression during myogenesis in the posthatch chicken establishes a model for satellite cell differentiation and renewal, *Dev. Dyn.*, **231**, 489–502.
45. Halevy, O., Yahav, S., and Rozenboim, I. 2006, Enhancement of meat production by environmental manipulations in embryo and young broilers, *World. Poultry Sci. J.*, **62**, 485–97.
46. Szabo, L., Morey, R., Palpant, N. J., et al. 2015, Statistically based splicing detection reveals neural enrichment and tissue-specific induction of circular RNA during human fetal development, *Genome Biol.*, **16**, 126.

47. Li, F., Zhang, L., Li, W., et al. 2015, Circular RNA ITCH has inhibitory effect on ESCC by suppressing the Wnt/beta-catenin pathway, *Oncotarget*, **6**, 6001–13.
48. Liu, Q., Zhang, X., Hu, X., et al. 2016, Circular RNA Related to the Chondrocyte ECM Regulates MMP13 Expression by Functioning as a MiR-136 'Sponge' in Human Cartilage Degradation, *Sci. Rep*., **6**, 22572.
49. Wang, K., Long, B., Liu, F., et al. 2016, A circular RNA protects the heart from pathological hypertrophy and heart failure by targeting miR-223, *Eur. Heart J*., **37**, 2602–11.
50. Yang, W., Du WW, Li, X., Yee, A. J., and Yang, B. B. 2016, Foxo3 activity promoted by non-coding effects of circular RNA and Foxo3 pseudogene in the inhibition of tumor growth and angiogenesis, *Oncogene*, **35**, 3919–31.
51. Zheng, Q., Bao, C., Guo, W., et al. 2016, Circular RNA profiling reveals an abundant circHIPK3 that regulates cell growth by sponging multiple miRNAs, *Nat. Commun*., **7**, 11215.
52. van Rooij, E., Liu, N., and Olson, E. N. 2008, MicroRNAs flex their muscles, *Trends Genet*., **24**, 159–66.
53. Townley-Tilson, W. H., Callis, T. E., Wang, D. 2010, MicroRNAs 1, 133, and 206: critical factors of skeletal and cardiac muscle development, function, and disease, *Int. J. Biochem. Cell Biol*., **42**, 1252–5.
54. Suzuki, H., Zuo, Y., Wang, J., Zhang, M. Q., Malhotra, A., and Mayeda, A. 2006, Characterization of RNase R-digested cellular RNA source that consists of lariat and circular RNAs from pre-mRNA splicing, *Nucleic Acids Res*., **34**, e63.
55. Nan, A., Chen, L., Zhang, N., et al. 2017, A novel regulatory network among LncRpa, CircRar1, MiR-671 and apoptotic genes promotes lead-induced neuronal cell apoptosis, *Arch. Toxicol*., **91**, 1671–84.
56. Liang, H. F., Zhang, X. Z., Liu, B. G., et al. 2017, Circular RNA circ-ABCB10 promotes breast cancer proliferation and progression through sponging miR-1271, *Am J Cancer Res*., **7**, 1566–76.
57. Jin, H., Jin, X., Zhang, H., and Wang, W. 2017, Circular RNA hsa-circ-0016347 promotes proliferation, invasion and metastasis of osteosarcoma cells, *Oncotarget*., **8**, 25571–81.
58. Elliman, S. J., Howley, B. V., Mehta, D. S., Fearnhead, H. O., Kemp, D. M., and Barkley, L. R. 2014, Selective repression of the oncogene cyclin D1 by the tumor suppressor miR-206 in cancers, *Oncogenesis*, **3**, e113.
59. Zhang, L., Liu, X., Jin, H., et al. 2013, miR-206 inhibits gastric cancer proliferation in part by repressing cyclinD2, *Cancer Lett*., **332**, 94–101.
60. Winbanks, C. E., Wang, B., Beyer, C., et al. 2011, TGF-beta regulates miR-206 and miR-29 to control myogenic differentiation through regulation of HDAC4, *J. Biol. Chem*., **286**, 13805–14.
61. You, X., Vlatkovic, I., Babic, A., et al. 2015, Neural circular RNAs are derived from synaptic genes and regulated by development and plasticity, *Nat. Neurosci*., **18**, 603–10.
62. Militello, G., Weirick, T., John, D., Doring, C., Dimmeler, S., and Uchida, S. 2017, Screening and validation of lncRNAs and circRNAs as miRNA sponges, *Brief. Bioinform*., **18**, 780–8.